

Implications of MRSI Compressed Sensing Reconstruction on Spatial Resolution Using a Modified Technique

Keith Wachowicz^{1,2}, Amr Heikal³, and B Gino Fallone^{2,4}

¹Oncology, University of Alberta, Edmonton, Alberta, Canada, ²Medical Physics, Cross Cancer Institute, Edmonton, Alberta, Canada, ³Physics, University of Alberta, Edmonton, Alberta, Canada, ⁴Physics and Oncology, University of Alberta, Edmonton, Alberta, Canada

Purpose:

The technique of compressed sensing (CS)¹ has generated significant interest in the MR community in recent years. This technique allows images to be generated with a dramatic reduction in acquired k-space data while retaining similar appearance to those conventionally acquired. However, there has been little quantitative scrutiny of this technique's potential impact on spatial resolution, which due to its non-linear reconstruction may be more difficult to discern on qualitative viewing than the uniform blur seen in low-resolution acquisitions. The aim of this work is two-fold: firstly, to quantitatively illustrate the impact of CS on spatial resolution using an implementation in spectroscopic imaging, and secondly to introduce a modified randomization and reconstruction algorithm to mitigate this impact. In this work, this modification is referred to as conjugate-mapped compressed sensing (CMaCS).

Theory:

Spectroscopic imaging is a technique that stands to benefit considerably from the use of CS. The frequent use of phase encoding in multiple encoding directions allows for great randomized decimation to acquired k-space. Reports of CS applied to ¹³C and ¹H spectroscopic imaging have investigated acceleration factors as high as 10.^{2,3} However, although the CS algorithm can reconstruct this under-sampled data with greatly reduced artifact, it is unlikely that spatial resolution does not suffer to some degree, especially at k-space frequencies with severe under-sampling. The modulation transfer function (MTF) is a metric that quantifies the amount of modulation at a specific frequency that is encoded in the output image, relative to input modulation at the same frequency.⁴ The MTF is normalized to 1 at zero frequency (uniform signal). For example, if an MRI were to image an object with a sinusoidally varying intensity, and the output image was only able to replicate the signal with an amplitude 80% that of the input (relative to the transfer of uniform signal), the MTF would record a response of 0.8 at that frequency. In this way, not only the limiting resolution can be quantified, but the ability of an imaging protocol to represent a complete range of spatial frequencies can be quantitatively recorded.

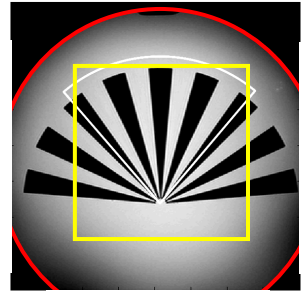


Figure 1. Fan phantom

Materials and Methods:

A phantom with a fan array of alternating 10° acrylic wedges and fluid-filled voids was constructed to allow for a square-wave input function (arc profile on fan structure) with continuous variation in spatial frequency (Fig. 1). The fan structure was immersed in a 6 mM choline, 20 mM creatine, and 25 mM acetate solution held in a 21 cm diameter cylinder (red outline). A 2D PRESS sequence with a 112 mm FOV (yellow outline), a 32x32 matrix, and a TR/TE of 1400/32 ms was implemented on a 3T Philips Intera platform. The resulting 32x32 matrix of spatial k-space data was 4x sub-sampled to represent a conventional lower-resolution scan (16x16), or with a randomized 1/r² probability distribution for CS. After reconstruction to a 128x128 grid, spectra for each pixel were analyzed to calculate acetate peak areas using in-house software.⁵ From the acetate area map, arc profiles over a range of radii were used to calculate the MTF at the corresponding spatial frequencies. This calculation compared the magnitude of the fundamental harmonic (evaluated through fourier transformation) to the magnitude of the input square wave. The zero frequency response was determined through the uniform fluid region underneath the fan structure, and this was used to normalize the resulting MTF response.

The CS reconstruction was based on the method outlined by Lustig et al.¹, using a 3D wavelet sparsity constraint. In both CS implementations, the k_x-k_y-t data was transformed to k_x-k_y-f before reconstruction. The CMaCS modification constrained the 1/r² randomization to avoid conjugate k-space replicas, and then prior to reconstruction a zero-order phase correction was independently performed on the 2D data set at each spectral frequency. This allowed the unpaired k-space conjugate locations to be estimated. Subsequently, the zero-order phase corrections were reversed before proceeding with the reconstruction.

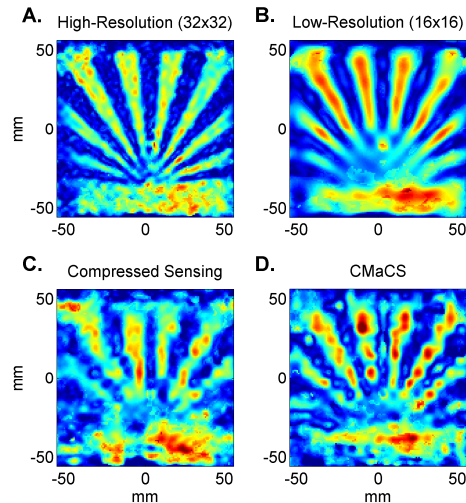


Figure 2. MRSI acetate maps derived with different sampling and reconstruction methods.

Results and Conclusions:

Measured acetate maps are displayed in Fig. 2, and the MTF responses for the different scenarios are shown in Fig. 3. It is clear from Fig. 3 that compressed sensing does not completely preserve the undersampled spatial frequencies. In fact, the response of higher spatial frequencies for the CS implementations here was markedly lower than the high-resolution 32x32 acquisition that they are intended to imitate (black plot). However, the CS reconstructions performed better than the time-equivalent low-resolution scan at high frequencies, at the cost of poorer response at low frequencies. The CMaCS algorithm (blue plot) performed much better than standard CS (magenta), with near two-fold increase in spatial frequency response above 0.8 cm⁻¹. Moreover, it did not suffer nearly as much at low-frequencies, and performed nearly as well on average as the time-equivalent 16x16 data set (red plot). The low frequency response of CMaCS does exhibit more instability than that of the 16x16 set, and this may originate from phase discontinuities from the conjugate mapping. Further, due to potential B₀ field variations across the FOV, a zero-order phase correction may be insufficient, and a more complex iterative phase-handling approach inside the CS operation may have to be implemented for increased robustness.

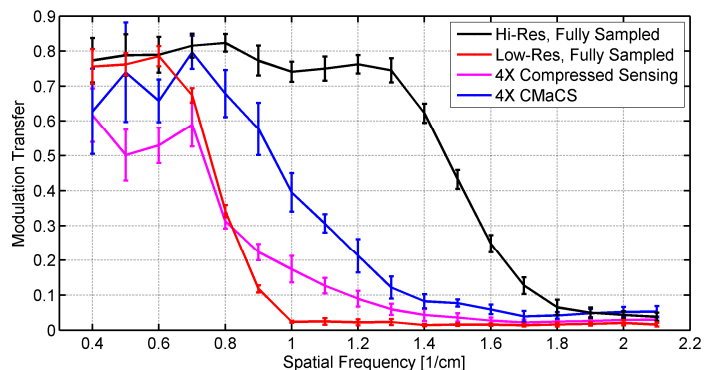


Figure 3. MTF response with different sampling / reconstruction methods

References: 1. Lustig et al. MRM 2007, p.1182; 2. Geethanath et al. Radiology 2012 (263), p.985; 3. Hu et al. MRM 2010, p.312; 4. Steckner et al. Med Phys 1994, p. 483; 5. Heikal et al. Radiol. Oncol. 2008, p.232

Acknowledgements: The authors would like to thank Philips Medical Systems for technical support in this work.